Received: 12 September 2023 | Revised: 7 November 2023 | Accepted: 13 November 2023

DOI: 10.1002/pts.2784

RESEARCH ARTICLE

Packaging Technology and Science
An International Journal

WILEY

Barrier, converting, and tray-forming properties of paperboard packaging materials coated with waterborne dispersions

Andrea Marinelli[1] | Johanna Lyytikäinen[2] | Panu Tanninen[2] | Barbara Del Curto[1] | Ville Leminen[2]

[1]Department of Chemistry, Materials and Chemical Engineering "Giulio Natta", Politecnico di Milano, Milan, Italy

[2]Lappeenranta-Lahti University of Technology LUT, Lappeenranta, Finland

Correspondence
Andrea Marinelli, Politecnico di Milano, Piazza Leonardo da Vinci 32, Milan 20131, Italy.
Email: andrea.marinelli@polimi.it

Abstract

In this work, different food-contact experimental and commercial aqueous polymeric dispersions were applied to paperboard via rod coating technology to achieve <5% non-cellulosic content. Barrier (water, moisture and grease), mechanical (tensile and bending) and converting (heat-sealing and creasing) properties were analysed before tray formation trials on pilot-scale equipment. Dispersion-coated samples were compared against polyethylene terephthalate (PET) extrusion-coated paperboard, the principal industrial material used for food trays. Results show that, within the investigated properties, waterborne dispersions can achieve similar barrier properties compared with PET, yet at lower dry coat grammage (12 g/m^2 vs. 40 g/m^2 of PET-coated paperboard). Additionally, the investigated coatings heat-sealed at temperatures as low as 80–90°C, almost 100°C less than PET; however, lower seal forces could be achieved (15–20 N/(25 mm) vs. 23 N/(25 mm) of PET-coated paperboard). Paperboard delamination occurred at the highest seal forces. Dispersion-coated trays were obtained at 4.5–5.0% blank moisture content. Formed trays at industrial processing parameters showed critical coating damage during converting due to tensile stresses. This work shows that milder processing conditions allow a reduction in coat defects.

KEYWORDS
aqueous dispersions, barrier properties, coating, converting, food packaging, mechanical properties, paperboard trays

1 | INTRODUCTION

Dispersion coating (DC) is an interesting technology that, despite being known for some decades, has only recently gained increased interest from the industry. Most of the commercialized coated fibre-based packaging is extrusion-coated or laminated. Only a few products are currently dispersion-coated[1]. One advantage of the DC technology is that it can achieve a lower final dry coat grammage compared with extrusion coating and lamination, reducing the non-cellulosic content of the packaging. This might lead to higher fibre recycling yields[2,3]. Indeed, previous studies[4–6] reported how DCs can be recycled, showing lower reject fractions. However, it was only recently that testing methodologies were standardized or developed for a European harmonization[7,8]; besides, such recycling methodologies are constantly adapting to address issues linked to the new packaging sold on the market. By potentially avoiding slot screening during recycling, thin coating and filler fragments might reach the secondary raw material (i.e., recycled material) or add up in the water circuits at the paper mill[9]. Related to microplastics, this potential issue is currently under discussion, possibly hindering the application of

numerous coatings that are brittle, fragment in tiny particles during repulping, and detach from fibres.

Previous studies focused on fillers[10–12] inside coating formulations and different latex polymeric nature, generally based on styrene-butadiene and styrene acrylates latexes[10–14]. Recent research focused on biobased polymers[15–19]; still, in many cases, they feature lower barrier properties as against synthetic counterparts, higher cost, and are challenging to scale up in their production process for an industrial technology transfer[20,21].

Nowadays, there are many commercially available aqueous dispersion grades, some of which were already applied and tested on paper substrates[22]. Most grades are based on synthetic latexes because of higher industrial availability and easier production processes, though academic and industry efforts to shift to bio-based counterparts must be acknowledged[15,16,23].

Besides a complete barrier properties characterization, the processing of fibre-based substrates might affect coating integrity, hence the final packaging performance[24–27]. Therefore, the evaluation of processing effects on the barrier properties, and the actual processability of such coatings is of extreme interest.

Creasing is a method that creates a groove in the processed material. It aims to locally decrease bending stiffness to generate preferential folding lines[28(p916)]. Different methods were reported to obtain creases, both in the flatbed die-cutting process[29,30] – commonly used in large-scale production – and with creasing wheels mounted on sample makers[30–32] to study, for example, both creasing patterns and crease orientation. Additionally, previous studies discussed the effect of crease rule and groove width on the processed material's thickness[29,32].

Heat-sealing, in contrast, is aimed at bonding two surfaces thanks to the action of temperature, pressure and time. Previous literature focused on both flexible[33,34] and rigid[35] packaging. Different seal bar geometries can be used, especially for flexible packaging, whereas rigid packaging commonly adopts a flat bar. A successful heat seal is required to ensure spill-proof packaging as well as sufficient adhesion to ensure unintentional package opening. Aqueous dispersions provide inferior heat-seal strength compared with laminated counterparts[36].

Multiple converting properties might be involved in a single forming process like paperboard 3D forming (referred to as drawing) to achieve a final packaging structure, for example, trays. Former studies explored several parameters affecting output quality, including packaging geometry, substrate moisture content, blank holding force, creasing depth and creasing width[31,35,37–39]. In summary, multiple process parameters must be finely tuned to guarantee that both the substrate and the coating layer do not crack; this would allow for a material-coating configuration that might compete under both economic and environmental perspectives against polymeric packaging counterparts, as well as against fibre-based solutions with higher non-cellulosic content.

In this work, the authors explored the production and characterization of both experimental mineral-filled and commercial aqueous dispersions on paperboard. The authors aimed for a broad characterization, going from barrier properties to converting properties and tray forming to be compared with polyethylene terephthalate (PET)-coated paperboard, currently the leading industrial material. This study involved dry dispersion coat grammages representing less than 5% of the total packaging weight, that is, maximum non-cellulosic content that might constitute an insignificant part of the packaging unit, hence possibly considered as monomaterial by EU member countries[40]. Therefore, the aim is to assess if and in which cases the use of lightweight DCs (<5% w/w non-cellulosic content) might substitute PET-coated substrates.

2 | MATERIALS AND METHODS

2.1 | Materials

2.1.1 | Substrate

StoraEnso (Helsinki, Finland) Trayforma 350 g/m^2 paperboard (UC) (average measured grammage was 348.5 g/m^2) was used as the basis substrate. UC is a three-layer 457 ± 4 μm thick bleached sulphate pulp paperboard, featuring chemithermomechanical pulp in the middle layer. All the layers are Alkyl Ketene Dimer (AKD) sized. Sizing improves the hydrophobic behaviour of the substrate.

Moreover, StoraEnso (Helsinki, Finland) Trayforma PET 40 extrusion-coated substrate (grammage: 350 + 40 g/m^2, UC + PET, respectively) (PET) was tested as reference commercial material, representing the commonest material used at an industrial scale to produce, for example, paperboard trays. The paperboard substrate of Trayforma PET 40 is UC.

2.1.2 | Experimental aqueous dispersions formulation

Two experimental formulations were produced at a lab scale involving HPH 39 highly crosslinked carboxylated styrene-butadiene latex ($T_g \cong 0°C$, dry solid content 54%) as binder – which was kindly provided by Trinseo (Horgen, Switzerland) – and CamCoat 80 kaolin (63% of the particles <2 μm in size) from Amberger Kaolinwerke (Hirschau, Germany) as filler:

- H39K 80, containing 80:20 latex: pigment ratio – dry weight ratio;
- H39K 60, containing 60:40 latex: pigment ratio – dry weight ratio.

Coating preparation followed the procedure described in previous publications[22,24]. PCC Exol SA (Brzeg Dolny, Poland) kindly provided Exolat C40 sodium polyacrylate, used as a dispersant (0.16% dry weight on dry pigment weight). NaOH 1 M was used to adjust the pH level to 8. At first, a water-based kaolin slurry was produced by adding kaolin powder, dispersant and NaOH inside deionized water. The slurry was continuously stirred with a turbine-type stirrer at 1200 rpm for at least 1 h. The final solid content of the slurry was 63%. Following, the kaolin slurry was mixed with HPH 39 latex (the amounts were according to the defined dry weight ratio) and stirred at 500 rpm for 30 min with the turbine type stirrer, adjusting the pH to 8 with NaOH. Experimental formulations had 50% solid content.

TABLE 1 Properties of the dispersion coatings involved in this study.

Coating	Solid content [%]	T_g [°C]	pH	Ford cup #4 viscosity [s]
H39K 80	50	0[a]	8	12
H39K 60	50	0[a]	8	11
SA-B	46	31.7	8	>60
SAP-H	51	12.1	7	18

[a]T_g of HPH 39 (neat latex used in the coating formulation).

Before any use, experimental formulations were stirred with a magnetic anchor for at least 1 h to ensure proper homogeneity. H39K 80 and H39K 60 were applied wet-on-wet to prepare double-layer coated samples.

2.1.3 | Commercial aqueous dispersions

In this work, two commercial aqueous dispersions were investigated. Such dispersions were already part of previous research for single-layer coated paper packaging[22,24]. Adopting a previous nomenclature, the specific grades studied in this context were:

- SA-B: styrene acrylate DC developed to provide barrier performance. Solid content is 46% (on a weight basis), whereas T_g is 31.7°C.
- SAP-H: heat-sealable styrene acrylate-based DC with 6% pigment by weight. Solid content is 51% (on a weight basis), whereas T_g is 12.1°C.

Considering a wet-on-wet double-layer coating investigation, three distinct configurations were produced and tested: SA-B, SAP-H and SAP-H over SA-B to make the coated substrates heat-sealable.

Table 1 reports the properties of both experimental and commercial DCs.

2.2 | Methods

2.2.1 | Sample preparation and preliminary characterization

The top side of UC was double coated along the machine direction (MD) using a 20 µm (wet film thickness) wire drawdown coater mounted on an Erichsen (Hemer, Germany) Coatmaster 510 automated coater. The machine was equipped with a vacuum suction plate to improve UC flatness on the coating plane. The coating speed was 50 mm/s, and no additional mass weighed on the coating rod. The second coat layer was applied wet-on-wet over the first one, that is, without oven-drying the first layer. Drying occurred in a VWR (Leuven, Belgium) Venti-line 180 Prime oven at 120°C for 90 s.

Unless elsewhere specified, coated samples were conditioned at 23 ± 1°C and 50 ± 2% relative humidity for at least 24 h before any further characterization and tests. The average dry coat grammage was determined as the difference between the grammage of the coated samples and the measured one of UC. The pinhole test was assessed according to the procedure defined in BS EN 13676:2001[41] with a 25 cm^2 testing apparatus. Five replicates were tested for each coating material. Additionally, Bendtsen roughness according to DIN 53108, and air permeability were measured using a Lorentzen & Wettre (Kista, Sweden) SE 114 Bendtsen Paper Roughness and Air Permeability Tester −10 measurements for each coating, as well as for UC. The pressure was 1.47 kPa for both roughness and air permeability tests; the latter was measured over an area of 10 cm^2.

A Biolin Scientific AB Attension Theta Optical Tensiometer (Göteborg, Sweden) was used to measure the sessile drop contact angle of both coated and uncoated substrates. A total of seven measurements were averaged for each sample. The deionized water droplet volume was 3 µl. The contact angle was measured 1 s after the application of the drop.

2.2.2 | Mechanical properties

A total of 20 samples (measuring 140 by 15 mm) – 10 alongside MD, and the same number alongside CD – were tensile tested according to BS ISO 1924-3:2005[42] using a Lorentzen & Wettre (Kista, Sweden) SE 064 Tensile tester. The testing length was 100 mm, whereas the crossheads speed was 100 mm/min.

A total of 20 samples (100 by 38 mm) – 10 alongside machine direction and the same amount alongside cross direction (CD) – were bending tested using a Lorentzen & Wettre (Kista, Sweden) SE 160 Bending Tester. The bending resistance (0–15°) and two-point bending stiffness (0–5°) were measured according to BS ISO 2493-1:2010[43] and ISO 5628:2019[44], respectively. For both tests, the bending length was 50 mm.

Before their testing, both grammage (see Section 2.2.1) and thickness were determined for both tensile and bending tests; the thickness was obtained using a Messmer Büchel (The Netherlands) 49–56 Micrometer, averaging 20 measurements.

2.2.3 | Barrier properties

Conditioned samples were tested for water absorptiveness (Cobb test), Water Vapour Transmission Rate (WVTR) and Oil and Grease Resistance (OGR).

Cobb 1800 (i.e., 30 min) test was performed according to the methodology defined in BS EN ISO 535:2014[45] on five samples over

an area of 25 cm^2. Water absorptiveness is defined as the weight increase of the sample due to water uptake during the test, divided by the testing area. The result is then converted to g/m^2. Lower water absorptiveness values indicate higher water barrier properties.

WVTR, instead, followed the evaluation procedure defined in BS ISO 2528:2017[46] using cups filled with 35.0 ± 0.1 g of silica gel. Three samples for each coating material were tested; the testing area was 20 cm^2. WVTR is defined as the amount of water vapour absorbed by silica gel at a steady state. It was calculated as the slope of mass increase in time, divided by the testing area. The result is reported in $g/(m^2 \cdot day)$. Lower WVTR values show higher water vapour barrier performance.

OGR followed a similar methodology to the one defined in BS ISO 16532-1:2008[47]. Evaluation times and setup were the same (50 g weights with a diameter of 30 mm), but the testing temperature was 60°C. This allowed harsher testing conditions for the substrates, simulating contact with hot greasy food. Given the temperature, dyed palm kernel oil was liquid, and the amount applied to the samples was 0.1 ml. A total of five samples for each coating were tested and the results were averaged. The outcomes were reported as defined in BS ISO 16532-1:2008[47].

2.2.4 | Creasing

Each aqueous dispersion configuration underwent creasing with a three-rule tool developed at LUT and already presented in a single-rule version in previous work[48]. The tool was mounted on a Shimadzu (Kyoto, Japan) Autograph AGS-X machine. It features three equally spaced 2 pt. (0.706 mm) rules that differ in length and whose corners are rounded — total length is almost 43 mm, excluding rounding. On the bottom, the authors used a 0.5 mm deep and 1.4 mm wide creasing matrix, leading to a creasing factor μ of 1.5 (see Tanninen et al.[32] for the equation to calculate μ).

The creasing pre-load was set to 10 N. The speed was constant at 5 mm/min for the pre-test and actual creasing. The authors assessed the effect of two different creasing strokes (0.5 mm and 0.6 mm, respectively) for both MD and CD fibre orientation of every double-coated layer configuration, leading to a crease depth of around 90–120 μm.

A Keyence (Osaka, Japan) VR-3200 wide-area 3D measurement system determined the real crease depth. For each sample, 11 multi-line profiles were equally spaced (0.5 mm distant) and averaged for each crease line.

Next, possible coating damage was evaluated through an OGR test, as described in Section 2.2.3. Five samples were tested for each creasing condition and each coating configuration. ORG testing of five uncreased samples provided reference resistance time.

2.2.5 | Heat sealing

An RDM Test Equipment (Hertfordshire, England) HSB-1 heat sealer was used to seal 25 by 130 mm coated strips with facing coated sides.

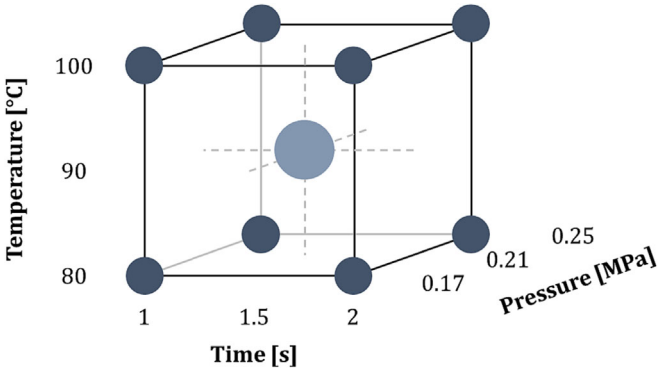

FIGURE 1 Heat sealing investigation matrix.

The equipment mounted flat 25 mm wide tools; the top one – moved by two pneumatic cylinders – was heated, whereas the bottom one, a flexible tool, was kept at room temperature.

A 2^3 full-factorial design of experiments (DoE) including a central point was designed adopting as variables temperature, dwell time and pressure. A schematic representation of such DoE is reported in Figure 1. The number of replicates was five. The reader should consider that the pressure in Figure 1 represents the cylinder pressure that allows a sample-specific pressure of 2, 2.5 and 3 MPa, respectively.

Heat-sealed samples were subsequently T-peel tested – unsupported peel testing, according to ASTM F88/F88M-21[49] – using a Shimadzu (Kyoto, Japan) Autograph AGS-X machine with pneumatic clamps. The pre-test speed was 50 mm/min until reaching 0.2 N. Afterwards, the speed was 300 mm/min until the end of the test. T-peel test curves were analysed to determine peak force, average force in the seal area, and peel energy in the seal area. Linear Pareto charts provided heat-sealing relevance for the analysed processing parameters. Since low dry coat grammages might negatively affect the heat-seal ability of rough substrates, the authors also considered the dry coat grammage of the single specimens as a factor to be included in Pareto charts. Indeed, the aim was to assess if small changes in the coat grammage could affect the heat-sealing performance.

2.2.6 | Tray forming

Tray forming behaviour was assessed for H39K 80, H39K 60, and SA-B + SAP-H coated paperboard. For comparison, the PET-coated paperboard was also investigated to ensure that the processing conditions corresponded to industrial production ones. Tray blanks were produced using commercial die-cutting equipment with 1/9 foodstuff container – nomenclature according to BS EN 631–1:1993[50] – die and matrix. Matrix groove width and depth were 1.4 mm and 0.5 mm, respectively; creasing rules were 2 pt. wide (0.706 mm) and 23 mm high, like for the creasing tests defined in Section 2.2.4. The crease pattern featured creases that were radial toward the rotation axis of the tray corner, as discussed in previous research[32]. The blanks were

FIGURE 2 Tray blank after creasing.

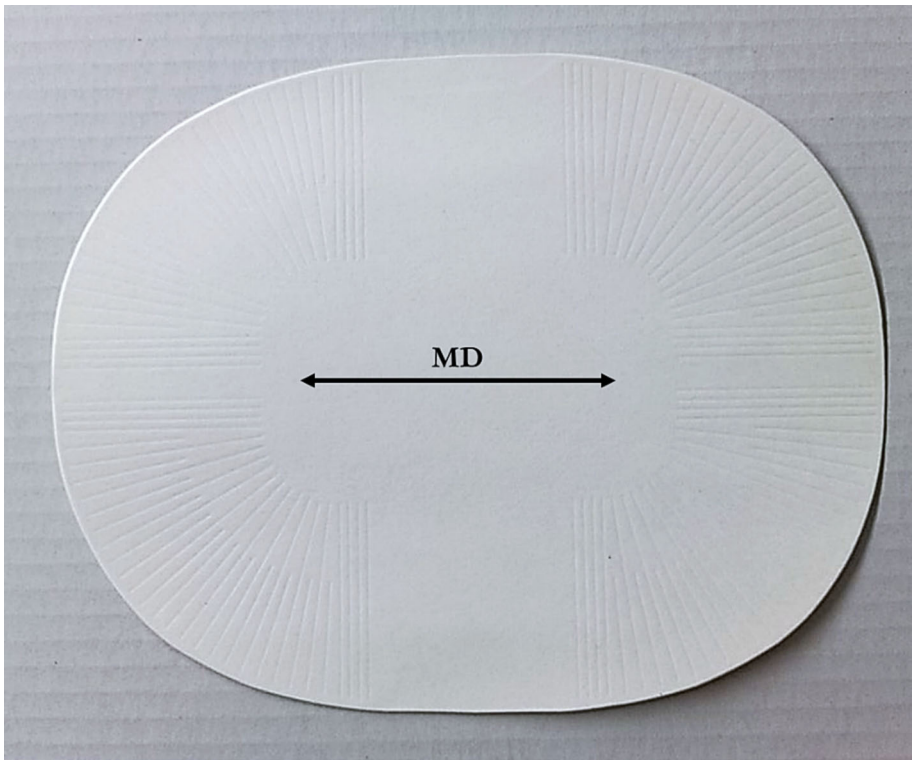

TABLE 2 Tray forming parameters.

Parameter	Units	Min	Max
Blank moisture content	[%]	4.0	5.6
Blank holding force	[kN]	0.546	1.014
Temperature	[°C]	100	120
Pressing speed	[mm/s]	45	90

Subsequently, coat defects due to press-formation were qualitatively evaluated using E131-dyed water and ethanol.

die-cut with the longer side aligned to the Machine Direction (MD) to provide higher tray stiffness (Figure 2).

Berry trays (142 mm × 94 mm × 50 mm) were press-formed from conditioned tray blanks, with main dimensions of 211.3 mm × 167.3 mm, varying blank moisture content (MC), blank holding force (BHF), temperature, and pressing speed — dwell time was constant to 0.6 s. PET blanks were formed maintaining the MC within the 8–9% range. The moisture content was assessed by testing ~5 g of material with an Adam Equipment (Milton Keynes, UK) PMB 53 Moisture Analyzer. Parameters ranged as reported in Table 2 and their effect was assessed following the previously mentioned sequence. Such specific order was because of preliminary tests, which showed a sticking behaviour of both H39K 80 and H39K 60. Dynamic friction tests at different MC (i.e., 2.4%, 7.4% and 11.0%, due to different conditioning environments) were performed on three samples for each coating, to be tested along MD. Dynamic friction equipment consisted of a 0.2 kg sled stuck to a sample-coated side facing a smooth stainless steel sliding plane.

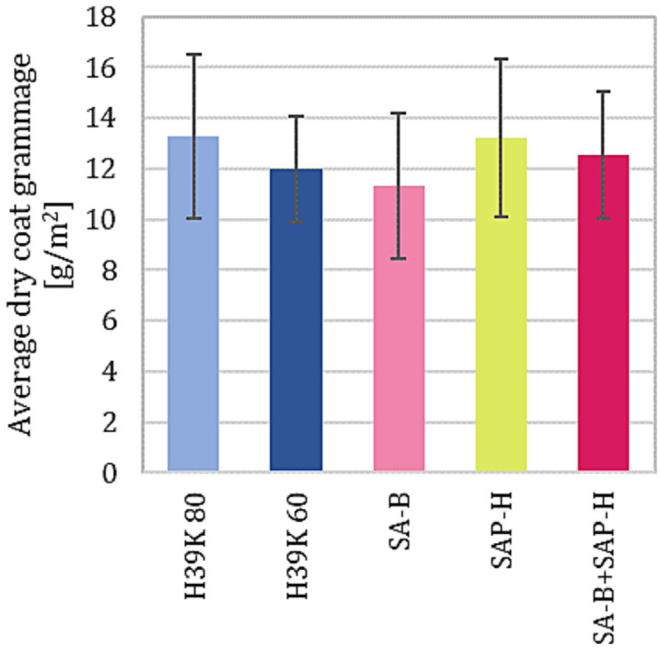

FIGURE 3 Average dry coat grammage for each coating investigated in this work.

2.2.7 | Statistical analysis

Graph representation was performed with MS Excel (all error bars represent standard deviation), whereas statistical analysis of the heat sealing experiments (see Section 2.2.5) was carried out using Minitab 21.3.1. Linear Pareto charts were produced to evaluate the relevance

TABLE 3 Average number of pinholes measured for each coating grade, both commercial and experimental.

Coating	Average number of pinholes
PET	0
H39K 80	2
H39K 60	0
SA-B	0
SAP-H	1
SA-B + SAP-H	0

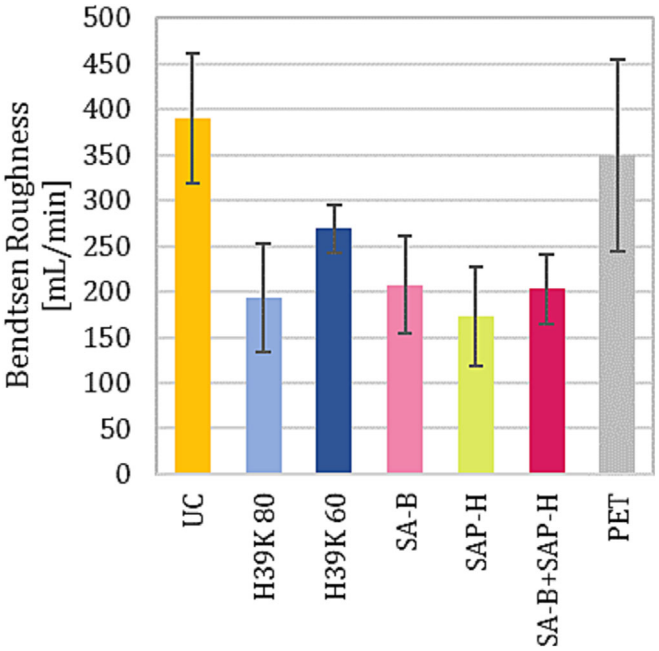

FIGURE 4 Bendtsen roughness of the coated side of different aqueous dispersion-coated paperboard. Uncoated and PET-coated paperboard are included, too.

of temperature, time, pressure and dry coat grammage processing parameters for heat-sealing.

3 | RESULTS

3.1 | Sample preparation and preliminary characterization

Coated paperboard was successfully obtained. Average dry coat grammages for each material under investigation are reported in Figure 3. Differently from what was expected, dry coat grammage for a double 20 µm wet thickness coating achieved an average of 12 g/m^2. This might be attributed to paperboard surface sizing, repelling to some extent the waterborne dispersion spread with the rod coater.

Generally, coated substrates showed few or no pinholes, as reported in Table 3. H39K 80 pinholes were explained by

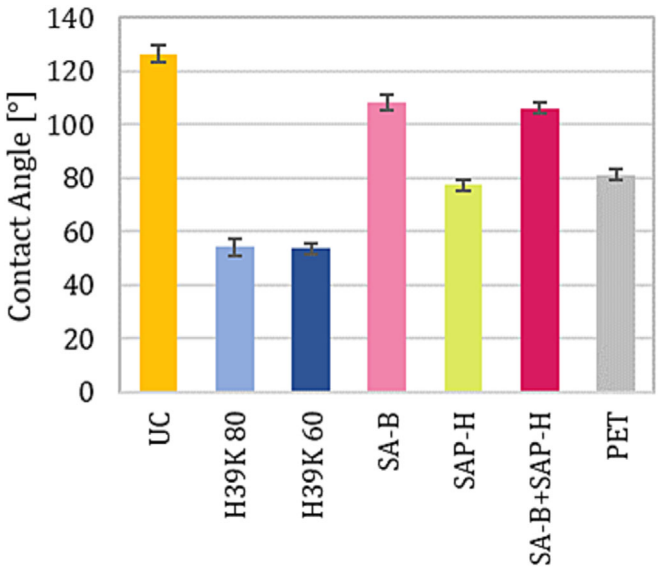

FIGURE 5 Dispersion-coated, uncoated, and PET-coated paperboard measured contact angle.

microbubbles incorporated in the aqueous dispersion during mixing since both experimental formulations feature no defoamers.

Bendtsen roughness is reported in Figure 4. UC and PET-coated samples achieved the highest results, whereas aqueous dispersions reached, on average, 200 ml/min roughness, meaning more than 55% reduction. It must be observed how, in general, H39K 60 showed higher Bendtsen roughness compared with H39K 80, which was attributed to increased kaolin content, which is coarser compared with latex particles that film-form[22,51].

Regarding air permeability, UC showed 4.23 ± 0.23 µm/(Pa·s) air permeability, whereas all the DCs and PET achieved results that were almost null (≤0.002 ± 0.001 µm/(Pa·s)).

Contact angle (Figure 5) clearly shows how experimental kaolin-containing styrene-butadiene coatings feature highly hydrophilic surface[52], without statistically significant difference due to different kaolin amounts. On the contrary, uncoated paperboard achieved the highest value (127°), highlighting the hydrophobic nature due to sizing agents. Interestingly, the SA-B + SAP-H coated paperboard featured a contact angle that was close to the SA-B one; this suggests that the wet-on-wet coating allows the two coating layer particles to interdiffuse before drying.

3.2 | Mechanical properties

Tensile and bending test results are reported in Figure 6 and Figure 7, respectively. The results differed depending on substrate fibre alignment, that is, MD or CD. MD alignment provided, as predictable, higher tensile strength, average maximum force, as well as bending resistance and stiffness due to parallel fibre alignment in tensile tests and orthogonal alignment to the bending axis—up to threefold values compared with CD.

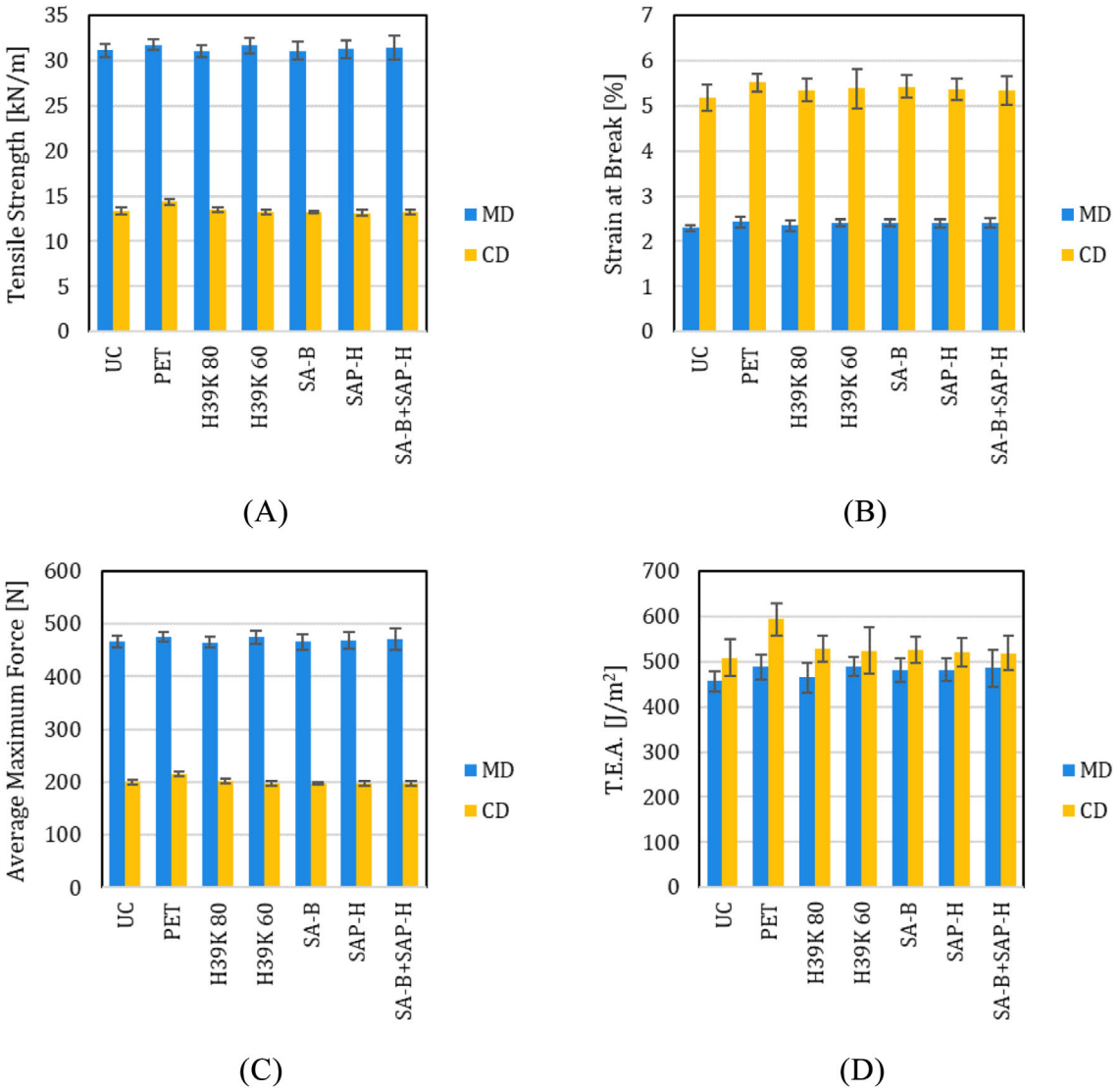

FIGURE 6 Tensile test results for both UC, PET, and dispersion-coated paperboard: a) tensile strength; b) strain at break; c) average maximum force; d) tensile energy absorption.

No significant difference could be observed in the investigated parameters because of different DC because of either close average value or standard deviation–as it is for bending stiffness (Figure 7.b). Such results are coherent with previous findings[53,54]. The rationale is in the low dry coat grammage compared with the substrate one, with the former accounting for less than 5% of the total grammage. The previous statement might be supported by the results for PET-coated substrate, generally showing better mechanical performance to both MD and CD. Indeed, the PET grammage fraction is slightly more than 10% of the total grammage.

3.3 | Barrier properties

Cobb1800 test results are reported in Figure 8. Experimental formulation provided minimal barrier compared with other coatings. Indeed, even SAP-H, a commercial heat-sealable grade, showed a water absorption that was 50% lower compared with H39K 80. On the other hand, SA-B achieved similar results compared with PET-coated paperboard, as well as SA-B + SAP-H coating configuration.

Coherently to previous studies[22,55–57], the presence of kaolin in the formulation proved to be of low benefit for improved water barrier properties because of its hydrophilic nature[58]. In particular, higher kaolin content generally led to increased water absorption. However, in terms of magnitude, such results differ from previous results[22,24] with the same coatings but different substrate, especially for experimental coatings, where higher dry coat grammage led to even worse relative performance.

WVTR (Figure 9), once again, showed how SA-B provided performances similar to PET (both less than 20 g/(m^2·day), whereas experimental formulations achieved results around 40 g/(m^2·day), with H39K 60 showing slightly lower WVTR, similarly to what described

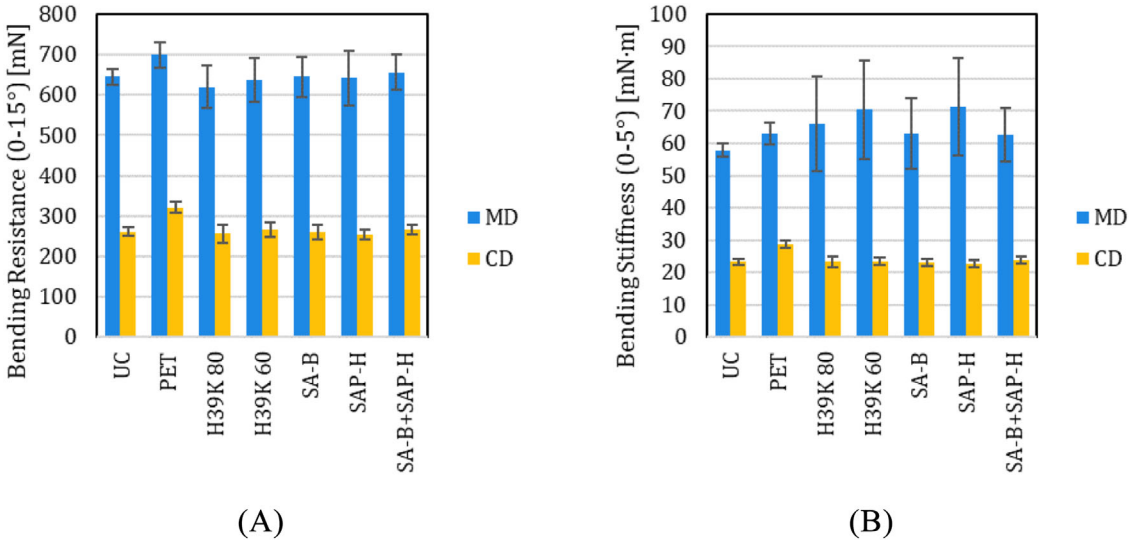

FIGURE 7 Bending test results for UC, PET, and dispersion-coated paperboard: a) bending resistance; b) bending stiffness.

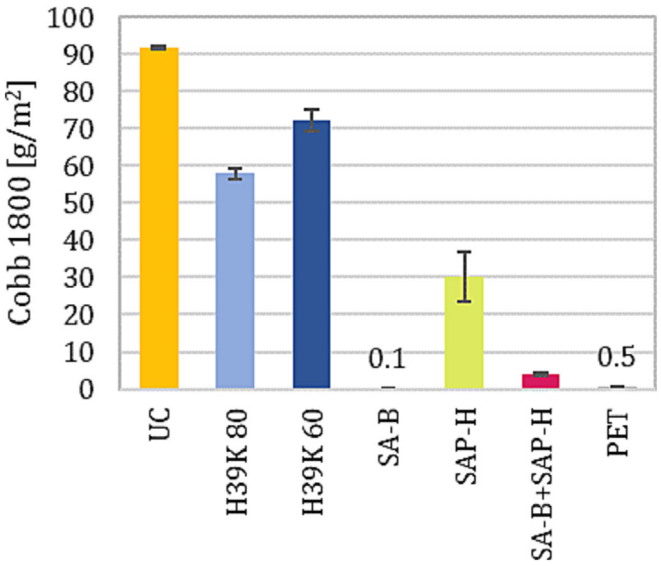

FIGURE 8 Water absorptiveness (Cobb1800 test) results of the investigated coatings.

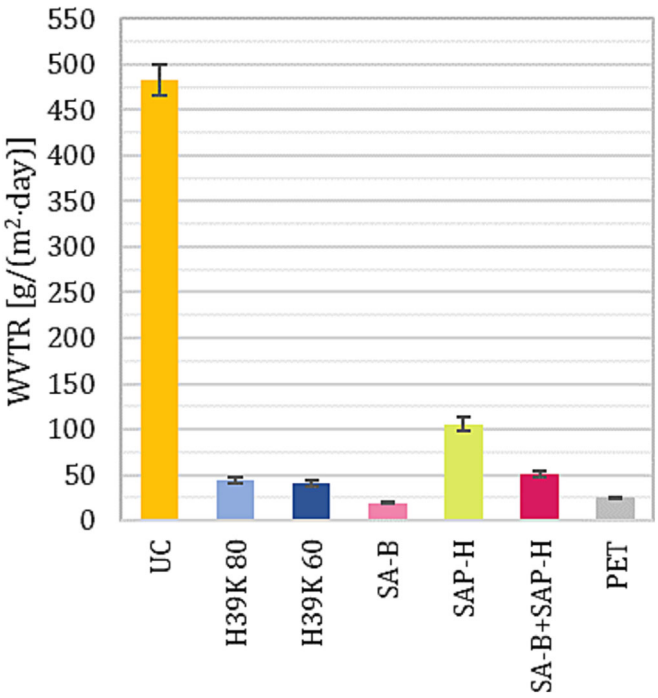

FIGURE 9 Moisture permeability (WVTR) results of the investigated coatings.

elsewhere[22]. Waterborne dispersions showed barrier properties improvement ranging from 80–95%. Still, coat weight should be considered when discussing results, since aqueous dispersions involved in this study led to less than half coat grammage than it was for PET. Both SA-B and experimental coatings achieved performance similar to previous studies with similar dry coat grammage[12,55,59].

Grease barrier resistance, expressed as minutes to spot dyed grease on the uncoated side of the samples, is reported in Table 4. UC samples showed no OGR. The oil penetrates through the material in a couple of seconds after its application on the surface. As a general statement, the different dispersions provided widely variably performance. Indeed, SA-B, which was the best-performing material for both water absorption and moisture barrier (Figure 8 and Figure 9, respectively) showed the worst resistance, only up to 4 h. On the contrary, both experimental formulations and SA-B + SAP-H configuration were able to resist up to 24 h at 60°C. Nonetheless, the best result, that is, similar to PET, was achieved with SAP-H, which was able to resist for more than 24 h.

Despite similar results achieved on paper substrates[22,24], the testing conditions involved in this research were harsher because of higher penetration rates caused by higher test temperature (i.e., 60°C instead of 23°C).

Overall, DCs achieved properties that were sometimes similar to PET, but at a reduced dry coat grammage. This means that, from a barrier point of view, dispersion-coated substrates might represent more sustainable solutions since they decrease the non-cellulosic content.

3.4 | Creasing

Results for creased samples are reported in Table 5, which also specifies failure mode. PET provided the best performance, alongside SAP-H; still, H39K 80 and H39K 60 showed interesting results, resisting between 6 and 24 h. PET sample was the only material that did not show dye colour leftovers on the coat side, highlighting that – at least to some extent – the coating absorbs dyed grease. Such results are coherent with similar previous literature[29].

Generally, samples failed because of general permeation through the coatings (Figure 10.c), suggesting once again the possible presence of pores that were filled by dyed grease. However, pores' dimension might be small, since colour was homogeneous and coat porosity was not observed at high magnification scanning electron microscope[22].

Nevertheless, as a general statement, samples were not affected by stroke or fibre orientation apart from SA-B + SAP-H, which failed because of several crease defects as of Figure 10.a and Figure 10.b. Such behaviour underlines a multi-DCs coat that is more brittle compared with aqueous dispersions used on their own. Single aqueous dispersions behaved similarly to extrusion-coated and laminated materials rather than cracking[60] at the studied crease depths. Therefore, crease stroke should be further reduced for SA-B + SAP-H, limiting creasing-induced defects. However, stroke reduction means – like increasing crease rule width – shallower creases, which are detrimental for leakproof seals[31,35]. Additionally, given the measured data, it seems that crease tip-related defects are more likely to be witnesses as against the ones along the crease line. The reason lies in crease rule tips, which generally undergo a filing process that might leave some dents that can damage thin coat layers more easily.

TABLE 4 Grease permeability of the investigated coatings. Unless specified, the results unit is minutes.

		Uncreased
UC	Test result	0
	Min-Max [min]	All <1
PET	Test result	>24 h
	Min-Max [min]	All >1440
H39K 80	Test result	6 < X < 24 h
	Min-Max [min]	All ≤1440
H39K 60	Test result	6 < X < 24 h
	Min-Max [min]	All ≤1440
SA-B	Test result	240
	Min-Max [min]	240–270
SAP-H	Test result	>24 h
	Min-Max [min]	All >1440
SA-B + SAP-H	Test result	6 < X < 24 h
	Min-Max [min]	All ≤1440

3.5 | Heat-sealing

Peel test results of heat-sealed samples are shown in Figure 11. H39K 60 and SA-B + SAP-H coated substrates behaved following the same trend, whereas H39K 80 did not vary as much as the others did. This

TABLE 5 Grease permeability of the investigated coatings after creasing. Different strokes and fibre orientation were considered. Additionally, failure modes are reported. Unless specified, the results unit is minutes.

	Stroke	0.5	0.5	0.6	0.6	
	Orientation	MD	CD	MD	CD	Failure mode
PET	Test result	>24 h	>24 h	>24 h	>24 h	n.a.
	Min-Max [min]	All >1440	All >1440	All >1440	All >1440	
H39K 80	Test result	6 < X < 24 h	6 < X < 24 h	6 < X < 24 h	6 < X < 24 h	Permeation through coating
	Min-Max [min]	All 1440	All 1440	All 1440	All 1440	
H39K 60	Test result	6 < X < 24 h	6 < X < 24 h	6 < X < 24 h	6 < X < 24 h	Permeation through coating (rare crease tip damage)
	Min-Max [min]	150–1440	330–1440	All 1440	150–1440	
SA-B	Test result	180	180	150	180	Permeation through coating
	Min-Max [min]	All 180	180–210	70–210	130–180	
SAP-H	Test result	>24 h	>24 h	>24 h	>24 h	n.a. (rare crease tip damage)
	Min-Max [min]	All >1440	All >1440	1440–> 1440	1440–> 1440	
SA-B + SAP-H	Test result	6 < X < 24 h	6 < X < 24 h	360	360	Crease tip damage (+some along crease)
	Min-Max [min]	180–1440	24–1440	30–1440	26–1440	

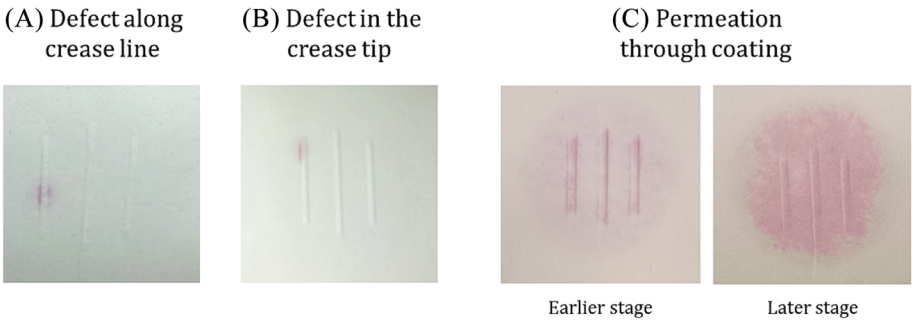

FIGURE 10 Pictures of the backside of the samples that show observed failure modes: a) coat defect along the crease line; b) coat defect because of the crease tip; and c) no coat defect because of creasing, but grease permeation through the coating.

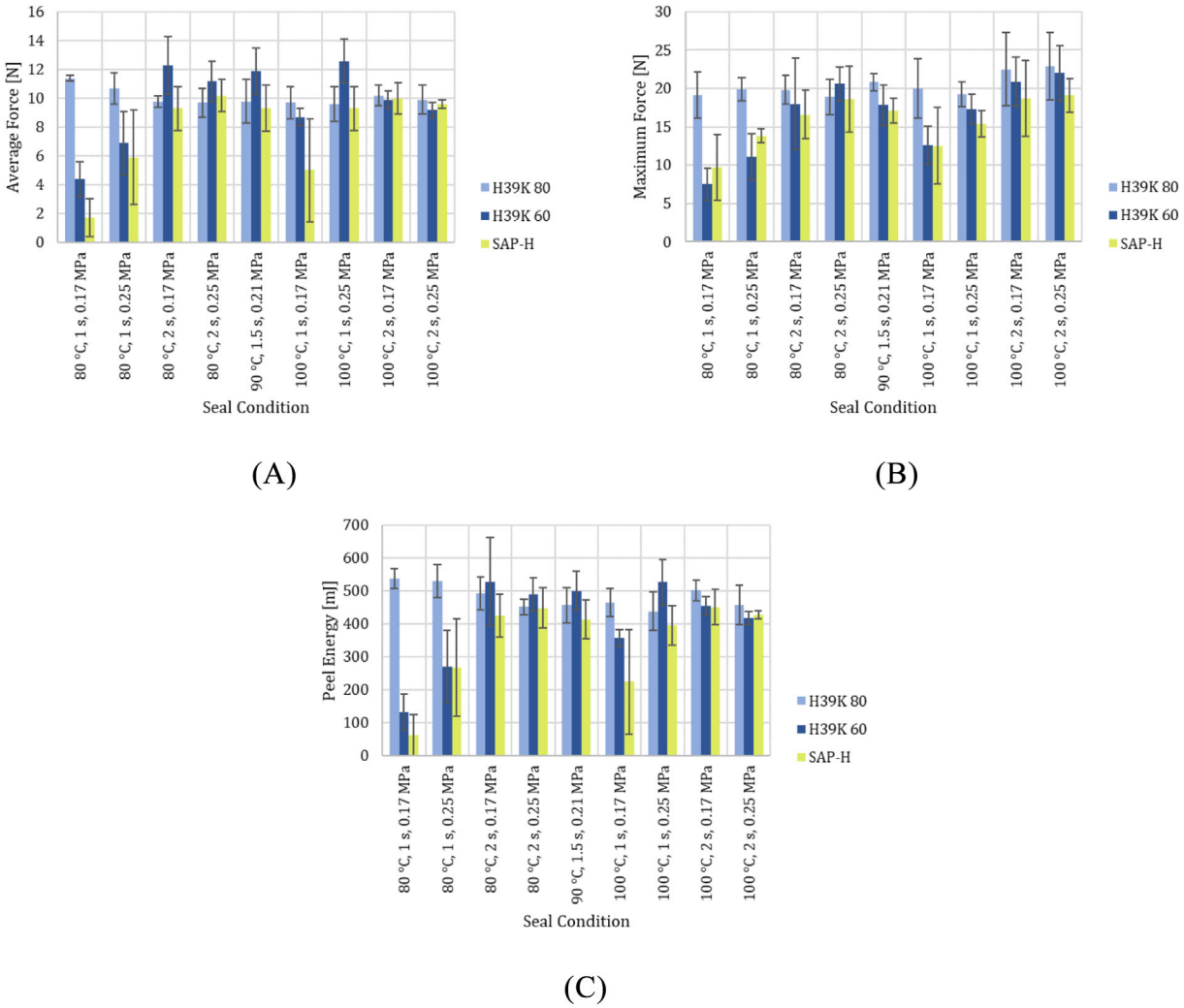

FIGURE 11 Peel test results for each heat-seal set of temperature, dwell time and pressure: a) average force; b) maximum force; c) seal energy.

might be explained by lower kaolin content that cannot shield native latex stickiness, as previously reported[24].

Similar to previous works[24,33], two main failure modes were retrieved: a separation along the coat-coat interface, and a crack formation in the sealant followed by paperboard delamination (i.e., fibre tear). Indicatively, the latter mode occurred at average forces ≥10 N — and, equivalently, to peel energies in the sealed area ≥450 mJ and maximum forces ≥18 N. Consequently, it could be stated how the ranges investigated in this work were not correct to spot out a change in H39K 80 behaviour, hence too high set of temperature, time and pressure. Additionally, peel energy values should not be considered meaningful when associated with paperboard delamination. The

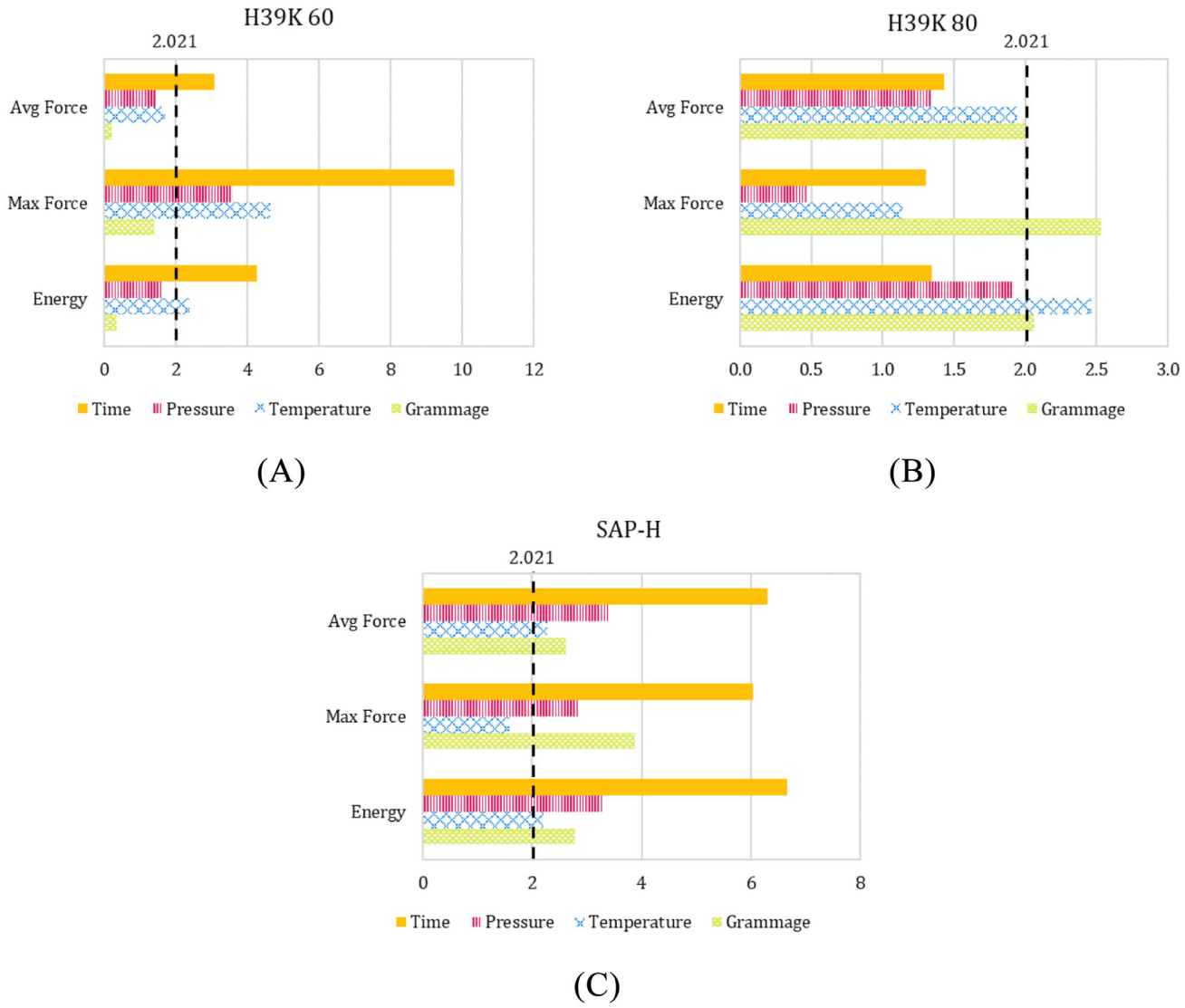

FIGURE 12 Linear Pareto charts of the standardized effects of heat-seal parameters, plus dry coat grammage: a) H39K 80; b) H39K 60; c) SAP-H. Factors with a score higher than the reference value (2.021, red dashed line) are statistically evident factors.

FIGURE 13 Maximum heat-seal force registered for samples sealed at different temperatures (dwell time: 1.5 s; equipment pressure: 0.21 MPa).

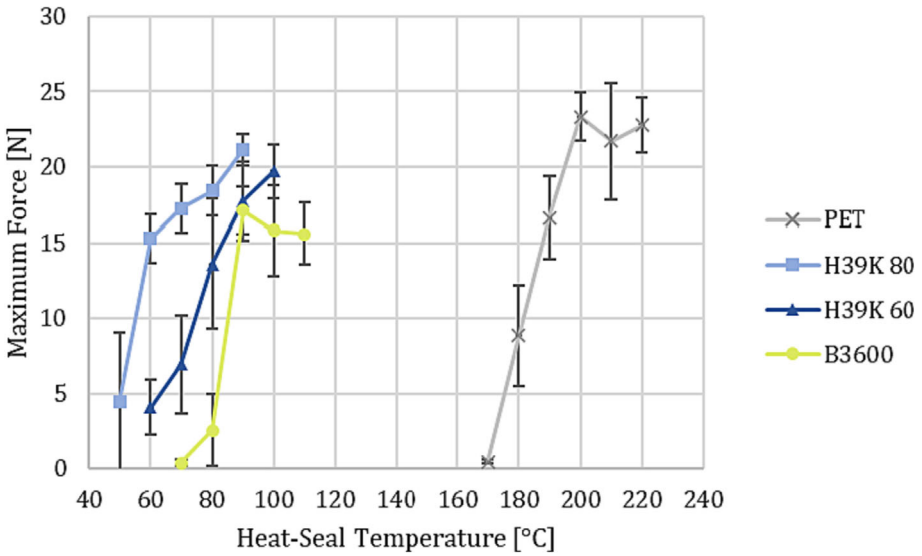

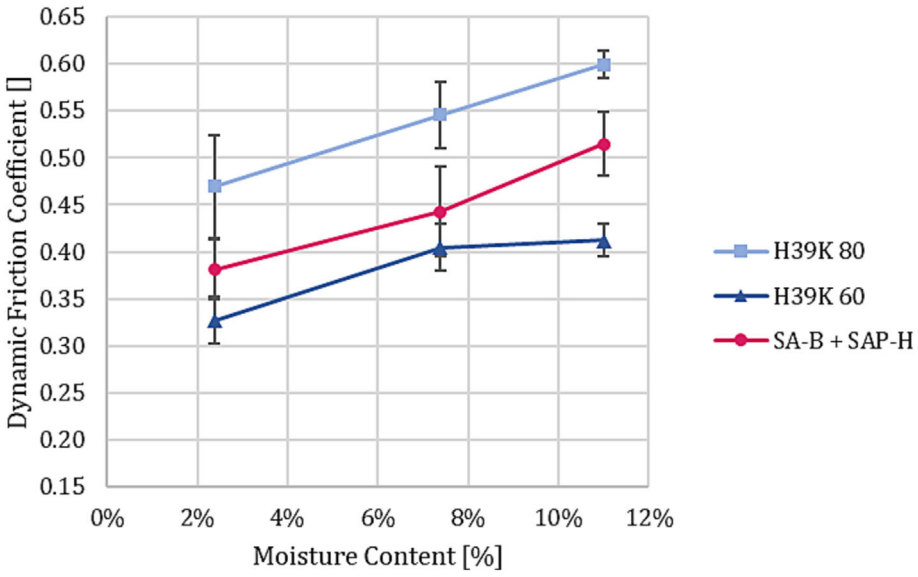

FIGURE 14 Dynamic friction results for H39K 80, H39K 60, and SA-B + SAP-H at different moisture contents.

reason lies in the energy contribution, which is not due to coat-to-coat interface separation; instead, the external energy provided by the system is mainly associated with fibre separation.

Linear Pareto charts for both processing parameters and dry coat grammage (Figure 12) highlight different statistically significant parameters for each material, given the same DoE. For H39K 80, it seems to be a matter of dry coat grammage. However, taking a closer look at the results for such coating (Figure 11), the change in sealing parameters appeared negligible in the measured outcomes. Indeed, almost every sample showed paperboard delamination (fibre tearing) during the peel test, underlining a coat-to-coat interface bonding that is stronger than the one of bulk paperboard, regardless of temperature, time and pressure applied during heat-sealing[34].

H39K 60 and SAP-H, instead, undoubtedly show the importance of time, plus temperature, notwithstanding the lower magnitude of the latter. Coherently with previous work[24] and despite higher substrate grammage (i.e., thickness), similar time range, and higher specific pressures (0.4 to 0.6 MPa versus 2 to 3 MPa of the current work), time was the most crucial parameter to obtain heat-sealed samples. The effect of time was discussed in previous work[33] to be crucial at lower temperatures because of thermal insulation properties of cellulosic substrates. As of Figure 11, data is coherent with such argument for all the investigated properties at 80°C and 100°C comparing samples sealed at 1 s and 2 s, with a sharper difference at lower sealing pressures. With a good approximation, also pressure was a significant parameter according to Pareto charts.

The authors compared the heat-seal ability of dispersion-coated paperboard with the one of PET-coated paperboard. As of Figure 13, maximum seal force clearly shows how aqueous dispersions are capable of sealing at temperatures that are around 100°C lower than PET ones. This represents a crucial advantage, leading to lower energy consumption, hence lowering production costs. Additionally, a major difference in peeling behaviour is that DCs generally fail by paperboard delamination, whereas PET separates at the coat-coat interface — despite some PET-paperboard interface bonding being damaged at higher temperatures. Higher maximum forces for PET-coated paperboard could be explained by the higher coat grammage – as well as the tough nature of the material – that provided higher Tensile Energy Absorption (Figure 6), that is, it was able to withstand peeling without breaking nor transferring the stress to paperboard fibres which, in turn, resists to a lower extent compared with coat–coat bond at the sealing interface (as observed for dispersion coated substrates). Recent research[36] showed how dispersion-

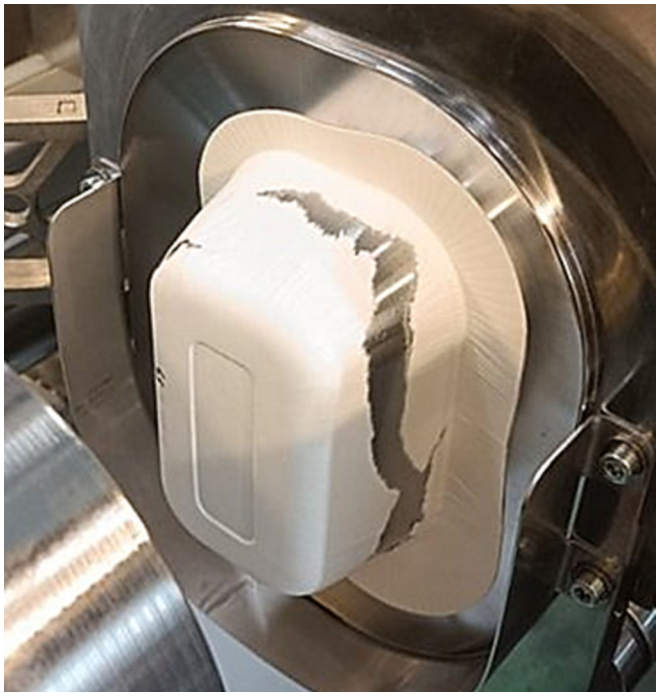

FIGURE 15 Blank breakage during tray forming. Higher moisture content increases friction, leading to blank adhesion to the male mould.

coated paper could withstand maximum forces that were almost 50% less than PE-coated similar substrates. In this work, the authors experienced similar behaviour, though the seal strength gap was considerably less, ranging from −10% to −20%. Although seal strength at a given set of sealing parameters is mainly driven by the polymeric nature, as well as possible pigment amount and fibre tear resistance, it should be considered that coat grammage might play a role in such lower strength, as suggested by Figure 12.c.

3.6 | Tray forming

Different materials showed different dynamic friction coefficients, as reported in Figure 14. It is clear how moisture plays a crucial role in determining the friction coefficient, with increasing MC leading to increased friction. Friction increased linearly with MC (for H39K 80 and SA-B + SAP-H, $R^2 \geq 0.98$) in the investigated moisture content range. Such behaviour might find a similar explanation as in previous research[33], since water increases paperboard thermal conduction, hence helping coating softening. Additionally, previous works discussed the hydroplasticizing effect of moisture on polymeric coating carboxyl groups, leading to reduced T_g[61,62]. H39K 80 and H39K 60 gap was explained by higher kaolin content, which reduced the equivalent latex (hence, fewer carboxyl groups) facing the sliding plane, thus limiting friction. The lower friction coefficient achieved by the presence of pigment is also coherent with previous findings[63,64]. Additionally, the friction coefficient was aligned with Bendtsen roughness values (Figure 4); indeed, H39K 60 features a rougher surface, hence fewer contact points to stick to the smooth steel surface.

Despite friction, coated paperboard trays were successfully achieved. The processing window in terms of MC for the experimental formulations was limited to ∼4.5–5.0%, whereas SA-B + SAP-H could be formed even at 5.6% — female mould: 100°C; BHF: 0.780 kN; pressing speed: 90 mm/s; dwell time: 0.6 s. Each coating material could not form at a lower MC (i.e., 4.0%). Such results differ from typical paperboard forming MC, which previous research reported to be around 8.0–9.0%[38,65,66]. Indeed, both trials at MC of 4.0% and preliminary tray forming at higher moisture content (>6.0%) showed highly adhesive behaviour on the male mould, which led to material breakage, as documented in Figure 15. Therefore, all the following processing was carried out at a blank MC of ∼4.5–5.0% for all the coatings involved.

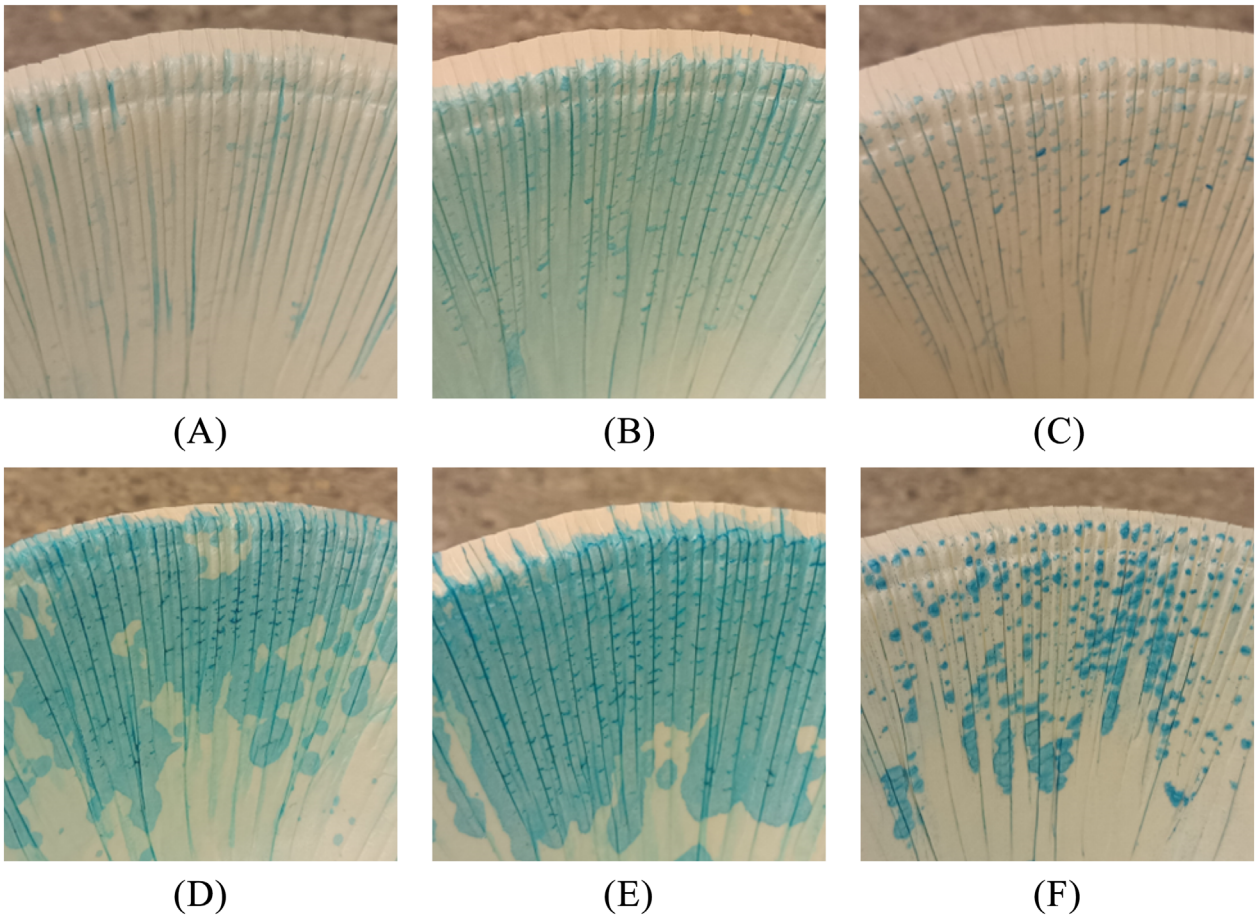

FIGURE 16 Dyed water and ethanol defects in the corners for H39K 80, H39K 60, and SA-B + SAP-H coated paperboard trays: a) H39K 80, water; b) H39K 60, water; c) SA-B + SAP-H, water; d) H39K 80, ethanol; e) H39K 60, ethanol; f) SA-B + SAP-H, ethanol. All trays were produced at 100°C, 0.780 kN BHF, 90 mm/s, 0.6 s dwell time.

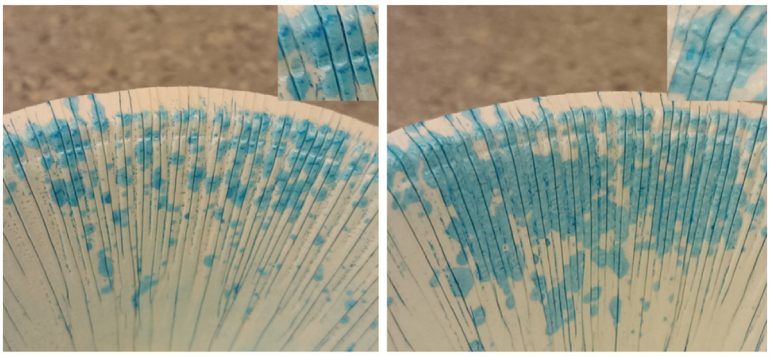

FIGURE 17 Effect of forming speed on coat defects for SA-B + SAP-H formed trays (dyed ethanol): a) 45 mm/s; b) 90 mm/s. Other forming parameters were 120°C, 1.014 kN BHF, and 0.6 s dwell time.

BHF is associated with friction, too. Increasing BHF leads to increased normal forces applied on the blank, hence friction. However, BHF is also proportional to the smoothness of the flange — which is, in turn, crucial for trays that need to be heat-sealed[35]. H39K 60 and SA-B + SAP-H could be processed at a BHF of 1.014 kN, whereas H39K 80 failed, badly sticking to the mould. Once again, higher pigment content seemed to help limit friction coefficient and stickiness.

The effect of processing temperature correlates to the thermal properties of the coatings. Higher mould temperature leads to increased chain mobility, which, in turn, helps the heat-sealing of the creases and adhesion to other substrates in general. SA-B + SAP-H trays were formed without any issues when mould temperature increased from 100°C to 120°C at both BHF of 0.780 kN and 1.014 kN. Similarly, H39K 80 and H39K 60 could be formed at 120°C at a BHF of 0.780 kN. Unfortunately, despite kaolin content, a BHF of 1.014 kN led to mould sticking for H39K 60 at 120°C. Additionally, both H39K 80 and H39K 60 were tray-formed at a BHF of 0.546 kN to have further data to assess forming speed.

From a material perspective, forming speed is primarily associated with deformation rate and latex softening (because of an extended contact time with the heated mould). The former, given other factors to be constant, influences the brittle or plastic behaviour of the coating, with higher speeds that can be associated with more fragile behaviour due to less time for the polymeric chains to flow without breaking. At 45 mm/s forming speed (120°C, BHF of 0.780 kN and 1.014 kN for SA-B + SAP-H, and 0.546 kN and 0.780 kN for H39K 80 and H39K 60), all the materials could be tray formed without sticking occurrence. Lower speed seemed to have a negligible effect on the adhesion and blocking effect of the investigated coated paperboard.

Despite successful tray forming at the given parameters' range, dyed water and ethanol generally highlighted quite damaged coatings (Figure 16). The main damaged areas were the corners and the flange. Specifically, the flange showed defects in the area exposed to tensile stresses (convex coated side), leaving fewer damages to the concave coated side. Moreover, despite lower sticking behaviour, H39K 60 was more damaged compared with H39K 80. The reason lies within lower latex continuity in highly pigmented formulations that lead to early breakage, similar to filled polymer matrix composites[67]. On the contrary, the PET sample trays showed no defects or sticking behaviour within the investigated parameter range, highlighting how the processing arrangement corresponded to the ones adopted for industrial production. Nonetheless, it must be noted that the PET coating was much thicker compared with dispersion-coated counterparts, allowing possible higher tensile resistance.

No marked difference was observed because of BHF and temperature parameter effects for the investigated ranges. Nevertheless, lower pressing speed showed significantly fewer defects, highlighting how higher speed helped damage the thin DCs (Figure 17). Additionally, taking a closer look at the defects, stained areas clearly show transversal cracks to the crease lines, suggesting damages caused by axial deformation.

4 | CONCLUSIONS

This work provided encouraging results from multiple points of view to sustain a narrow yet possible material substitution to reduce non-cellulosic content in paperboard-based packaging.

SA-B aqueous dispersion provided water and moisture barrier properties that were similar to PET, whereas SAP-H for grease barrier. Experimental dispersions, on the contrary, featured intermediate values, apart from water barrier properties. Nevertheless, the results were satisfying because of the lower dry coat grammage involved for dispersions as against PET.

The investigated creasing depth range did not affect the coating integrity of both experimental formulations (i.e., H39K 80 and H39K 60) and SAP-H, generally leaving grease permeation values intact. Some damages were observed with SA-B and SA-B + SAP-H, highlighting a more fragile behaviour at room temperature.

Aqueous dispersion-coated paperboard could be heat sealed at temperatures that were up to 100°C lower compared with conventional PET-coated paperboard, representing a better choice to reduce power consumption. Such behaviour appeared to be proportional to the T_g of each polymeric fraction. Despite lower seal strength, such materials may be used in applications where a temperature-sensitive content is involved. Unfortunately, the peel mechanism for strongly sealed samples was paperboard delamination, suggesting early coating breakage, whereas PET separates at the heat-sealed interface.

Paperboard dispersion-coated trays could be manufactured; however, moisture content was reduced to 4.5–5.0% to prevent blanks from sticking to the equipment. Although this is an atypical procedure to prepare the materials for processing, it strongly affected coating blocking behaviour. Still, tray forming speed damaged coat integrity. Lower formation speed and higher temperature proved to qualitatively reduce coat cracking, though fine-tuning is required to achieve a flawless converted coated paperboard tray. Overall, dispersion-coated substrates showed good machinability.

The present study provided further insights into the relationship between coating properties and their influence on process parameters, posing an additional basis for future research.

ACKNOWLEDGEMENTS

The authors would like to thank the companies for supplying materials as well as Antti Pesonen for assisting in the laboratory experiments.

DATA AVAILABILITY STATEMENT

The data that support the findings of this study are available from the corresponding author upon reasonable request.

ORCID

Andrea Marinelli https://orcid.org/0000-0002-2646-8686
Johanna Lyytikäinen https://orcid.org/0000-0002-2241-762X
Panu Tanninen https://orcid.org/0000-0001-6570-5253
Barbara Del Curto https://orcid.org/0000-0002-0125-0226
Ville Leminen https://orcid.org/0000-0001-5854-3321

REFERENCES

1. Marinelli A, Sossini L, Santi R, Del Curto B. *Imballaggio Cellulosico Con Proprietà Barriera: Stato Dell'arte e Innovazione Dei Materiali*. 1st ed. Edizioni Dativo Srl; 2022. https://www.comieco.org/downloads/16177/9158/STAMPATO-Imballaggio cellulosico con proprieta barriera.pdf
2. Bakker S, Kloos J, Metselaar GA, Catarina A, Esteves C, Schenning APHJ. About gas barrier performance and recyclability of waterborne coatings on paperboard. *Coatings*. 2022;12(12):1841. doi:10.3390/COATINGS12121841
3. Chi K, He J, Lin W-S, Bokhari SMQ, Catchmark JM. Electrostatically complexed natural polysaccharides as aqueous barrier coatings for sustainable and recyclable fiber-based packaging. *ACS Appl Mater Interfaces*. 2023;15(9):12248-12260. doi:10.1021/acsami.2c17886
4. Andersson C. New ways to enhance the functionality of paperboard by surface treatment - a review. *Packag Technol Sci*. 2008;21(6):339-373. doi:10.1002/PTS.823
5. Lee TJ, Yoon C, Ryu JY. A new potential paper resource; recyclability of paper cups coated with water-soluble polyacrylate-based polymer. *Nord Pulp Pap Res J*. 2017;32(1):155-161. doi:10.3183/npprj-2017-32-01-p155-161
6. Ovaska S-S, Sami-Seppo K, Lyytikäinen J, Hirn U, Backfolk K. Determination of Repulpability of Talc-Filled Biopolymer Dispersion Coatings and Optimization of Repulped Reject for Improved Material Efficiency by Tailoring Coatings. In: *Tappi PaperCon 2017 proceedings*; 2017:36-48. doi:10.2/JQUERY.MIN.JS
7. UNI. *UNI 11743*:2019. http://store.uni.com/catalogo/uni-11743-2019?josso_back_to=http://store.uni.com/josso-security-check.php&josso_cmd=login_optional&josso_partnerapp_host=store.uni.com. Accessed July 2, 2019.
8. Cepi. *Harmonised European laboratory test method to generate parameters enabling the assessment of the recyclability of paper and board products in standard paper and board recycling mills*.; 2022. https://www.cepi.org/cepi-recyclability-test-method-version-2/
9. Zhang H, Bussini D, Hortal M, Elegir G, Mendes J, Jordá BM. PLA coated paper containing active inorganic nanoparticles: material characterization and fate of nanoparticles in the paper recycling process. *Waste Manag*. 2016;52:339-345. doi:10.1016/j.wasman.2016.03.045
10. Martinez-Hermosilla GA, Mesic BB, Bronlund JE. Relative permeability of barrier dispersion coatings applied on paper-based materials; mathematical modeling and experimental validation. *J Coatings Technol Res*. 2022;19(2):543-558. doi:10.1007/S11998-021-00552-3/FIGURES/13
11. Mesic BB, Cairns M, Järnstrom L, Joo Le Guen M, Parr R. Film formation and barrier performance of latex based coating: impact of drying temperature in a flexographic process. *Prog Org Coat*. 2019;129:43-51. doi:10.1016/J.PORGCOAT.2018.12.025
12. Schuman T, Karlsson A, Larsson J, Wikström M, Rigdahl M. Characteristics of pigment-filled polymer coatings on paperboard. *Prog Org Coat*. 2005;54(4):360-371. doi:10.1016/J.PORGCOAT.2005.06.017
13. Kimpimäki T, Savolainen AV. Barrier dispersion coating of paper and board. In: Brander J, Thron I, eds. *Surface application of paper chemicals*. Springer; 1997:208-228. doi:10.1007/978-94-009-1457-5_12
14. Marinelli A, Diamanti MV, Lucotti A, Pedeferri MP, Del Curto B. Evaluation of coatings to improve the durability and water-barrier properties of corrugated cardboard. *Coatings*. 2022;12(1):10. doi:10.3390/COATINGS12010010
15. Coltelli MB, Wild F, Bugnicourt E, et al. State of the art in the development and properties of protein-based films and coatings and their applicability to cellulose based products: an extensive review. *Coatings*. 2015;6(1):1. doi:10.3390/COATINGS6010001
16. Rastogi VK, Samyn P. Bio-based coatings for paper applications. *Coatings*. 2015;5:887-930. doi:10.3390/coatings5040887
17. Kathuria A, Zhang S. Sustainable and Repulpable barrier coatings for fiber-based materials for food packaging: a review. *Front Mater*. 2022;9:9. doi:10.3389/fmats.2022.929501
18. Tyagi P, Salem KS, Hubbe MA, Pal L. Advances in barrier coatings and film technologies for achieving sustainable packaging of food products – a review. *Trends Food Sci Technol*. 2021;115:461-485. doi:10.1016/j.tifs.2021.06.036
19. Wang J, Euring M, Ostendorf K, Zhang K. Biobased materials for food packaging. *J Bioresour Bioprod*. 2022;7(1):1-13. doi:10.1016/j.jobab.2021.11.004
20. Wu F, Misra M, Mohanty AK. Challenges and new opportunities on barrier performance of biodegradable polymers for sustainable packaging. *Prog Polym Sci*. 2021;117:101395. doi:10.1016/J.PROGPOLYMSCI.2021.101395
21. Nilsen-Nygaard J, Fernández EN, Radusin T, et al. Current status of biobased and biodegradable food packaging materials: impact on food quality and effect of innovative processing technologies. *Compr Rev Food Sci Food Saf*. 2021;20(2):1333-1380. doi:10.1111/1541-4337.12715
22. Marinelli A, Diamanti MV, Pedeferri MP, Del Curto B. Kaolin-filled styrene-butadiene-based dispersion coatings for paper-based packaging: effect on water, moisture, and grease barrier properties. *Coatings*. 2023;13(1):195. doi:10.3390/COATINGS13010195
23. Cazón P, Velazquez G, Ramírez JA, Vázquez M. Polysaccharide-based films and coatings for food packaging: a review. *Food Hydrocoll*. 2017;68:136-148. doi:10.1016/J.FOODHYD.2016.09.009
24. Marinelli A, Profaizer M, Diamanti MV, Pedeferri M, Del Curto B. Heat-seal ability and fold cracking resistance of kaolin-filled styrene-butadiene-based aqueous dispersions for paper-based packaging. *Coatings*. 2023;13(6):975. doi:10.3390/coatings13060975

25. Oh K, Sim K, Bin JY, et al. Effect of coating binder on fold cracking of coated paper. *Nord Pulp Pap Res J*. 2015;30(2):361-368. doi:10.3183/npprj-2015-30-02-p361-368
26. Yang A, Xie Y, Renjung W. From Theory to Practice: Improving the Foldcrack Resistance of Industrially Produced Triple Coated Paper. In: *Papercon*; 2011:1845-1858.
27. Zhu Y, Bousfield D, Gramlich WM. The influence of pigment type and loading on water vapor barrier properties of paper coatings before and after folding. *Prog Org Coat*. 2019;132:132-210. doi:10.1016/j.porgcoat.2019.03.031
28. Holik H. *Handbook of paper and board*. Wiley-VCH Verlag GmbH & Co. KGaA; 2013. doi:10.1002/9783527652495
29. Tanninen P, Leminen V, Lindell H, Saukkonen E, Backfolk K. Adjusting the die cutting process and tools for biopolymer dispersion coated paperboards. *Nord Pulp Pap Res J*. 2015;30(2):336-343. doi:10.3183/npprj-2015-30-02-p336-343
30. Leminen V, Niini A, Tanninen P, Matthews S. Comparison of creasing and scoring in the manufacturing of folding cartons. *Procedia Manuf*. 2021;55(C):221-225. doi:10.1016/J.PROMFG.2021.10.031
31. Leminen V, Matthews S, Tanninen P, Varis J. Effect of creasing tool dimensions on the quality of press-formed paperboard trays. *Procedia Manuf*. 2018;25:397-403. doi:10.1016/J.PROMFG.2018.06.109
32. Tanninen P, Leminen V, Eskelinen H, Lindell H, Varis J. Controlling the folding of the blank in paperboard tray press forming. *BioResources*. 2015;10(3):5191-5202. doi:10.15376/biores.10.3.5191-5202
33. Hauptmann M, Bär W, Schmidtchen L, et al. The sealing behavior of new mono-polyolefin and paper-based film laminates in the context of bag form-fill-seal machines. *Packag Technol Sci*. 2021;34(2):117-126. doi:10.1002/PTS.2544
34. Merabtene M, Tanninen P, Varis J, Leminen V. Heat sealing evaluation and Runnability issues of flexible paper materials in a vertical form fill seal packaging machine. *BioResources*. 2022;17(1):223-242. doi:10.15376/BIORES.17.1.223-242
35. Leminen V, Mäkelä P, Tanninen P, Varis J. Leakproof heat sealing of paperboard trays - effect of sealing pressure and crease geometry. *BioResources*. 2015;10(4):6906-6916. doi:10.15376/biores.10.4.6906-6916
36. Merabtene M, Tanninen P, Wolf J, et al. Heat-sealing and microscopic evaluation of paper-based coated materials using various seal bar geometries in vertical form fill seal machine. *Packag Technol Sci*. 2023;36(8):667-679. doi:10.1002/PTS.2735
37. Hauptmann M, Majschak J-P. New quality level of packaging components from paperboard through technology improvement in 3D forming. *Packag Technol Sci*. 2011;24(7):419-432. doi:10.1002/pts.941
38. Niini A, Berthold L, Müller T, et al. Effect of blank moisture content on forming behaviour and mechanical properties of paperboard tray packages. *J Appl Packag Res*. 2022;14(1):1-18. https://scholarworks.rit.edu/japr/vol14/iss1/4/
39. Östlund M, Borodulina S, Östlund S. Influence of paperboard structure and processing conditions on forming of complex paperboard structures. *Packag Technol Sci*. 2011;24(6):331-341. doi:10.1002/pts.942
40. European Commission. *Commission implementing decision (EU) 2019/665*. https://eur-lex.europa.eu/legal-content/EN/TXT/?uri=CELEX%3A32019D0665. 2019. Accessed February 3, 2022.
41. BS EN 12702. *Adhesives for paper and board, packaging and disposable sanitary products. Determination of blocking behaviour of potentially adhesive layers*. BSOL British Standards Online. https://bsol.bsigroup.com/Bibliographic/BibliographicInfoData/000000000030019633. Published 2000; 2000. Accessed November 15, 2022
42. BS ISO 1924-3. *Paper and board. Determination of tensile properties. Constant rate of elongation method (100 mm/min)*. BSOL British Standards Online. https://bsol.bsigroup.com/Bibliographic/BibliographicInfoData/000000000030102136. Published 2005; 2005. Accessed April 18, 2023
43. BS ISO 2493-1. *Paper and board. Determination of bending resistance. Constant rate of deflection*. BSOL British Standards Online. https://bsol.bsigroup.com/Bibliographic/BibliographicInfoData/000000000030190546. Published 2010; 2010. Accessed April 18, 2023
44. BS ISO 5628. *Paper and board. Determination of bending stiffness. General principles for two-point, three-point and four-point methods*. BSOL British Standards; 2019. https://bsol.bsigroup.com/Bibliographic/BibliographicInfoData/000000000030379994. Published 2019
45. BS EN ISO 535. In: BSOL British Standards Online, ed. https://bsol.bsigroup.com/Bibliographic/BibliographicInfoData/000000000030259603. Published 2014*Paper and board. Determination of water absorptiveness. Cobb method*; 2014. Accessed January 5, 2021
46. BS ISO 2528. *Sheet materials. Determination of water vapour transmission rate (WVTR). Gravimetric (dish) method*. BSOL British Standards Online. https://bsol.bsigroup.com/Bibliographic/BibliographicInfoData/000000000030349864. Published 2017; 2017. Accessed March 3, 2022
47. BS ISO 16532-1. *Paper and board. Determination of grease resistance. Permeability test*. BSOL British Standards Online. https://bsol.bsigroup.com/Bibliographic/BibliographicInfoData/000000000030164327. Published 2008; 2008. Accessed February 2, 2022
48. Tanninen P, Matthews S, Leminen V, Varis J. Analysis of paperboard creasing properties with a novel device. *Procedia Manuf*. 2021;55:232-237. doi:10.1016/j.promfg.2021.10.033
49. ASTM. *ASTM F88/F88M-21. Standard test method for seal strength of flexible barrier materials*. https://www.astm.org/f0088_f0088m-21.html. Published 2021. Accessed February 2, 2023.
50. BS EN 631–1. *Materials and articles in contact with foodstuffs. Catering containers. Specification for dimensions of containers*. BSOL British Standards Online. https://bsol.bsigroup.com/Bibliographic/BibliographicInfoData/000000000000319214. Published 1993; 1993. Accessed May 5, 2023
51. Al-Turaif H. Surface coating properties of different shape and size pigment blends. *Prog Org Coat*. 2009;65(3):322-327. doi:10.1016/J.PORGCOAT.2009.01.001
52. Järnström J, Väisänen M, Lehto R, Jäsberg A, Timonen J, Peltonen J. Effect of latex on surface structure and wetting of pigment coatings. *Colloids Surfaces a Physicochem Eng Asp*. 2010;353(2–3):104-116. doi:10.1016/j.colsurfa.2009.11.001
53. Türe H, Gällstedt M, Johansson E, Hedenqvist MS. Wheat-gluten/montmorillonite clay multilayer-coated paperboards with high barrier properties. *Ind Crop Prod*. 2013;51:1-6. doi:10.1016/j.indcrop.2013.08.054
54. Havimo M, Jalomäki J, Granström M, et al. Mechanical strength and water resistance of paperboard coated with long chain cellulose esters. *Packag Technol Sci*. 2011;24(4):249-258. doi:10.1002/pts.932
55. Zou Y, Hsieh JS, Mehnert E, Kokoszka J. The effect of pigments and latices on the properties of coated paper. *Colloids Surfaces a Physicochem Eng Asp*. 2007;294(1–3):40-45. doi:10.1016/J.COLSURFA.2006.07.046
56. Popil RE. Optimizing water resistance of linerboard coatings using pigments. *Tappi J*. 2006;5(9):18-26.
57. Thitsartarn W, Jinkarn T. Water resistance improvement of paperboard by coating formulations based on nanoscale pigments. *J Coatings Technol Res*. 2020;17(6):1609-1617. doi:10.1007/S11998-020-00386-5/FIGURES/10
58. Lyons A, Reed G. Pigmented aqueous barrier coatings. *TAPPI j*. 2020;19(11):551-558. doi:10.32964/TJ19.11.551

59. Kugge C, Johnson B. Improved barrier properties of double dispersion coated liner. *Prog Org Coat*. 2008;62(4):430-435. doi:10.1016/J.PORGCOAT.2008.03.006
60. Poulose S, Toriseva J, Lahti J, Jönkkäri I, Hedenqvist MS, Kuusipalo J. A green high barrier solution for paperboard packaging based on potato fruit juice, poly (lactic acid), and poly (butylene adipate terephthalate). *ACS Appl Polym Mater*. 2022;4(6):4179-4188. doi:10.1021/acsapm.2c00153
61. Bakker S, Aarts J, Esteves ACC, Metselaar GA, Schenning APHJ. Water barrier properties of resin-stabilized waterborne coatings for paperboard. *Macromol Mater Eng*. 2022;307(4):2100829. doi:10.1002/mame.202100829
62. Voogt B, Huinink H, van de Kamp-Peeters L, et al. Hydroplasticization of latex films with varying methacrylic acid content. *Polymer (Guildf)*. 2019;166:206-214. doi:10.1016/J.POLYMER.2019.01.074
63. Hubbe MA, Gill RA. Fillers for papermaking: a review of their properties, usage practices, and their mechanistic role. *BioResources*. 2016;11(1):2886-2963. doi:10.15376/biores.11.1.2886-2963
64. Rättö P, Barbier C, Rigdahl M. An investigation of the friction properties of coated paper. *Nord Pulp Pap Res J*. 2000;15(5):351-356. doi:10.3183/npprj-2000-15-05-p351-356
65. Kettle J. Moisture and fluid transport. In: Niskanen K, ed. *Paper physics (papermaking science and technology)*. 2nd ed. Finnish Paper Engineers' Association/Paperi ja Puu Oy; 2008:265-294.
66. Tanninen P, Lindell H, Saukkonen E, Backfolk K. Thermal and mechanical durability of starch-based dual polymer coatings in the press forming of paperboard. *Packag Technol Sci*. 2014;27(5):353-363. doi:10.1002/pts.2036
67. Faruk O, Bledzki AK, Fink HP, Sain M. Biocomposites reinforced with natural fibers: 2000-2010. *Prog Polym Sci*. 2012;37(11):1552-1596. doi:10.1016/j.progpolymsci.2012.04.003

How to cite this article: Marinelli A, Lyytikäinen J, Tanninen P, Del Curto B, Leminen V. Barrier, converting, and tray-forming properties of paperboard packaging materials coated with waterborne dispersions. *Packag Technol Sci*. 2023;1-17. doi:10.1002/pts.2784